

Simulated ECG Waveforms in Long QT Syndrome Based on a Model of Human Ventricular Tissue

KQ Wang¹, YF Yuan¹, YY Tang¹, H Zhang²

¹Harbin Institute of Technology, Harbin, China

²University of Manchester, Manchester, UK

Abstract

The electrocardiogram (ECG) is an important index of clinical diagnosis of cardiac arrhythmias. Simulations of ECG had revealed the causative relationship between waveforms of ECG and action potentials (APs). However, those studies were mainly based on the Luo-Rudy (LRd) model or the Priebe-Beuckelman (PB) model. In this study, we developed a 1D model of transmural ventricular strand based on the Tusscher et al. (TNNP) model of human ventricular myocytes. Using the model, the computed QT interval is 335 ms under the control condition. The value fits well with the clinical diagnosis (320~440 ms) and is about 100 ms longer than that from the LRd model. We studied the ECG waveforms under the LQT condition due to various ionic channel gene mutations. The morphology of simulated ECG resembles the main features of clinical recorded ECG of LQT syndrome, which include prolongation of the QT interval, widening of T wave, and increasing of the amplitude of T wave. This study provides an important insight to understand the causative link between LQT syndrome and underlying genetic mutations.

1. Introduction

The electrocardiogram (ECG) plays a significant role in diagnosis and treatment of cardiac arrhythmias, whereas analysis and interpretation of electrocardiographic waveforms remains mostly empirical. Previous studies [1-3] used an electrophysiological model of ventricular cardiac cell to study the possible relationship between waveforms of ECG and APs under various conditions, and succeeded in establishing the pseudo-ECG for long-QT syndrome (LQT), Brugada syndrome and acute ischemia with corresponding changes in individual ion channels and AP properties. These studies were mostly based on the LRd or the PB model (the LRd model is for guinea pig ventricular cells and the PB model is mostly based on the LR II model). However, animal hearts may differ significantly from human hearts in terms of features of electrical activity, such as AP

shape, duration, and restitution, tissue's vulnerability to arrhythmias. The TNNP model [4] is a novel human ventricular model and almost all its major ionic currents are based on recent experimental data obtained from human cardiac myocytes. Compared to the LRd and the PB models, the computed APD₉₀ from the TNNP model is about 270 ms, which fits better to experimental measurement [5], as shown in Fig.1. In this study, we developed a 1D model of transmural ventricular strand with the TNNP model. Using the model, we simulated the waveforms of ECG for various types of LQT syndrome. The results of simulated ECG are closely to the experimental and clinical observed records.

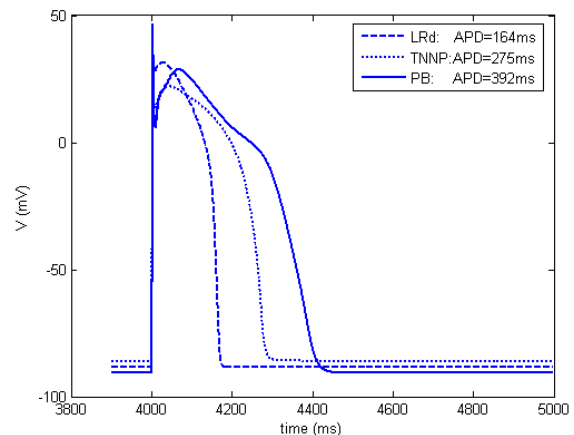


Figure 1. APs computed from the LRd, the TNNP and the PB models. The measured APD₉₀s of the three models are 164 ms, 275 ms and 392 ms respectively. APD₉₀ is defined as the duration of APs at 90% repolarization.

2. Methods

2.1. Modelling action potentials

Heterogeneous action potentials of epicardial (EPI), mid-myocardial (MID) and endocardial (ENDO) ventricular cells were modeled by the same approach as used by Tusscher et al. In the model, G_{Ks} is the maximal conductance of ionic channel current I_{Ks} and was set to 0.245 nS/pF for EPI cell, 0.062 nS/pF for MID cell

(EPI $\times 7/23$) and 0.149 nS/pF for ENDO cell (EPI $\times 14/23$). The maximal conductance G_{K_r} of I_{K_r} was same for the three cell types (0.096 nS/pF). The value of G_{T_o} (maximal conductance of ionic channel current I_{T_o}) was set to 0.294 nS/pF for EPI and MID cells, but 0.073 nS/pF for ENDO cell. APs of the three cells were produced under the same stimuli, which had a basic cycle length of 1000ms and the strength and duration of each stimulus are $-20 \mu\text{A}/\text{cm}^2$ and 2 ms respectively. Fig.2 shows the waveforms of APs of the three cells at the fifth stimulus, since APDs are relatively steady after this stimulus.

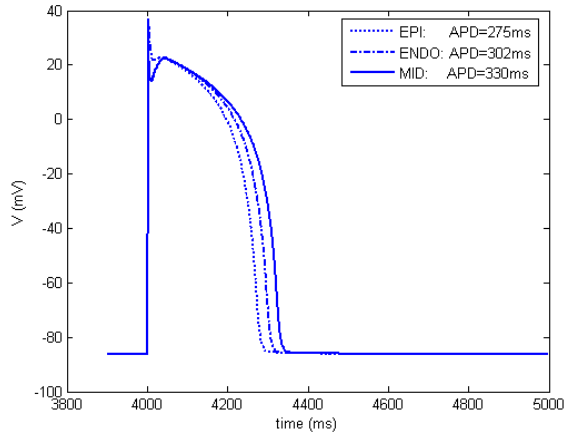


Figure 2. Simulated APs for EPI, ENDO and MID cells. The measured APD_{90s} are 275 ms, 302 ms and 330 ms respectively.

2. 2. One dimensional strand model

A 1D model of transmural ventricular strand was developed by incorporating the single cell models into a diffusion partial differential equation:

$$\frac{\partial V}{\partial t} = -\frac{I_{ion} + I_{stim}}{C_m} + D \cdot \frac{\partial^2 V}{\partial x^2} \quad (1)$$

Where V is transmembrane voltage, t time, I_{ion} the sum of all transmembrane ionic currents, I_{stim} the density of stimulus current, C_m cell capacitance per unit surface area, D the diffusion coefficient of the intercellular electrical coupling via gap junctions, and x is the spatial position at the 1D strand. C_m was set to $2.0 \mu\text{F}/\text{cm}^2$ and D was set to $0.00154 \text{ cm}^2/\text{ms}$ as defined by [2]. The length and proportions of the simulated 1D strand were same with those used by Gima and Luo [1]. The computed strand, which had a total length of 1.65 cm, was composed of 165 cells, which employed 60 cells for EPI cell, 45 cells for MID cells, and 60 cells for ENDO cell.

2. 3. Computing the pseudo-ECG

The pseudo-ECG was generated at a hypothetical

“electrode”, which was at a position 2.0 cm away from the last epicardial cell along the fiber axis. Extracellular unipolar potential is computed by the following equation:

$$\phi_e(x') = \frac{a^2 \delta_i}{4\delta_e} \int (-\nabla V_m) \cdot \left(\nabla \frac{1}{r} \right) dx \quad (2)$$

$$r = |x - x'|$$

where ∇V_m is the spatial gradient of transmembrane potential V_m , a is the radius of the 1D strand, δ_e and δ_i are respectively the extracellular and intracellular conductivity, and r is distance from a source point x to a field point x' . All parameters of the equation are as same as those defined in [1].

In Fig.3, wave propagation and the computed pseudo-ECG generated by the equations (1,2) are illustrated. Because of differences in transmural APDs and timings of depolarization and repolarization along the strand, the simulated pseudo-ECG presents a QRS wave followed by a positive T wave, which is similar to clinical recordings.

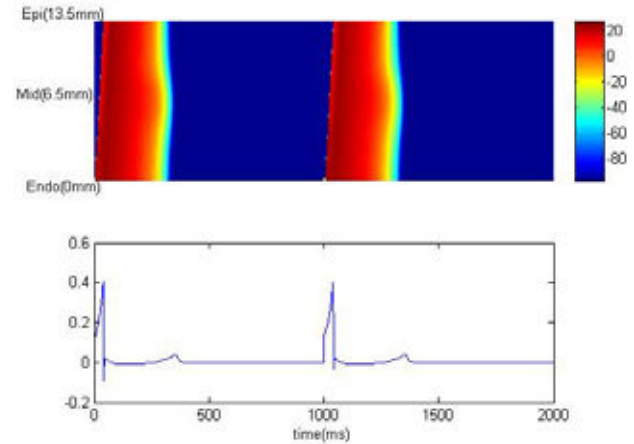


Figure 3. Propagation of excitation wave on the 1D transmural strand and corresponding pseudo-ECG.

3. Results

Fig.4 shows the simulated ECGs using the TNNP model, which are compared to the LRd model. The computed QT interval is 335 ms for the TNNP model and is 206 ms for the LRd model. As there are no PB EPI, PB MID and PB ENDO cell models, we did not incorporate transmural heterogeneity in a PB strand model. The QT interval generated by a homogeneous PB strand model is about 470 ms under the control condition, which is far larger than 320~440 ms of the normal QT interval of human recorded clinically. So the study based on the TNNP model is more suitable to investigate human cardiac disease (specially related to the QT interval changes) than the LRd and the PB models.

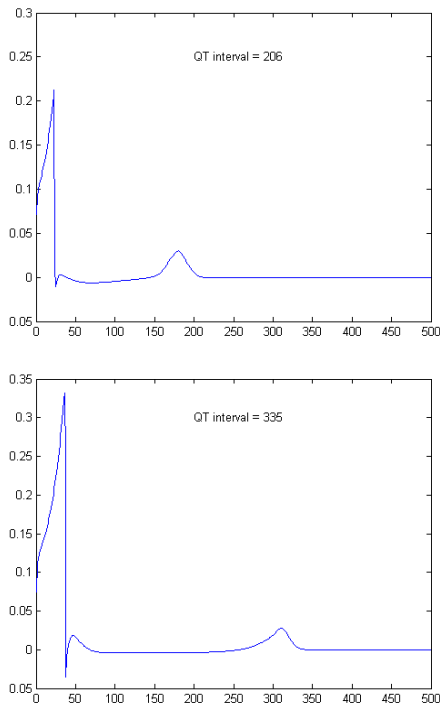


Figure 4. Comparison of the QT intervals of the LRd model and the TNNP model (LRd = 206 ms and TNNP = 335 ms).

Evidence [6] suggests that KVLQT1 gene mutation links to LQT1 and results in a reduction of the slow rectifying potassium current I_{Ks} ; HERG gene mutation relates to LQT2 and causes a reduction of the rapid rectifying potassium current I_{Kr} and SCN5A gene mutation is responsible for LQT3, which results in a “gain of function” abnormality with a persistent inward sodium current in the plateau phase of action potential. In simulations, we blocked I_{Ks} to 50%, 25% and 0% of its normal value to simulate LQT1 whilst blocked I_{Kr} to 50%, 25% and 0% of its normal value to model LQT2. In LQT3 simulation, a persistent inward sodium current in the plateau phase of action potential was added to the model with its amplitude being 0.1%, 0.15% and 0.2% of the peak value of the fast sodium current I_{Na} .

Fig.5-Fig.7 show the simulated pseudo-ECGs under LQT1, LQT2 and LQT3 settings. The simulated pseudo-ECGs present some typical morphologic features of LQT syndrome, such as prolongation of the QT interval, widening of the T wave duration and enlargement of the T-wave amplitude (except LQT1). Our simulated QT intervals are smaller than the clinical data [7], which are 470 ± 40 ms, 470 ± 30 ms and 500 ± 50 ms respectively for LQT1, LQT2 and LQT3. However, our simulations illustrate closely the relationship between the waveforms of ECG and the APs under various LQT syndrome conditions.

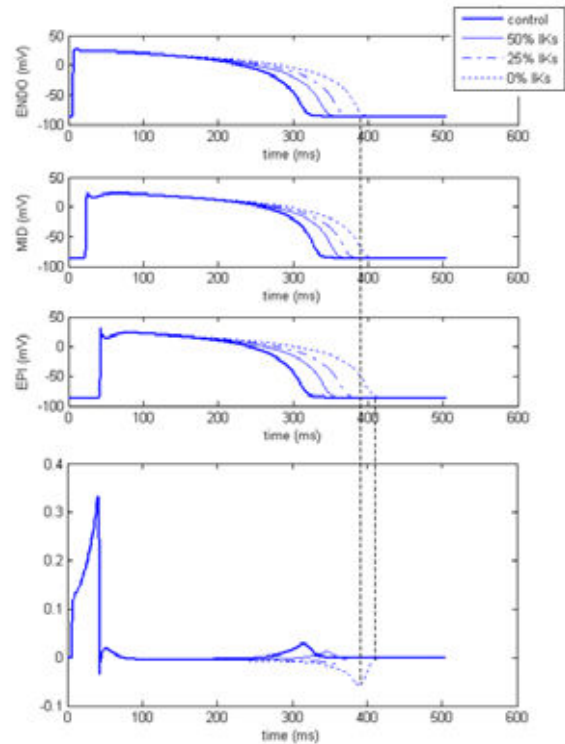


Figure 5. QT intervals of LQT1 on the ECG are prolonged (control = 335 ms, $50\%I_{Ks} = 361$ ms, $25\%I_{Ks} = 373$ ms and $0\%I_{Ks} = 408$ ms), but changes of the T waves are not clear, even there is an inverted T wave when I_{Ks} is blocked totally.

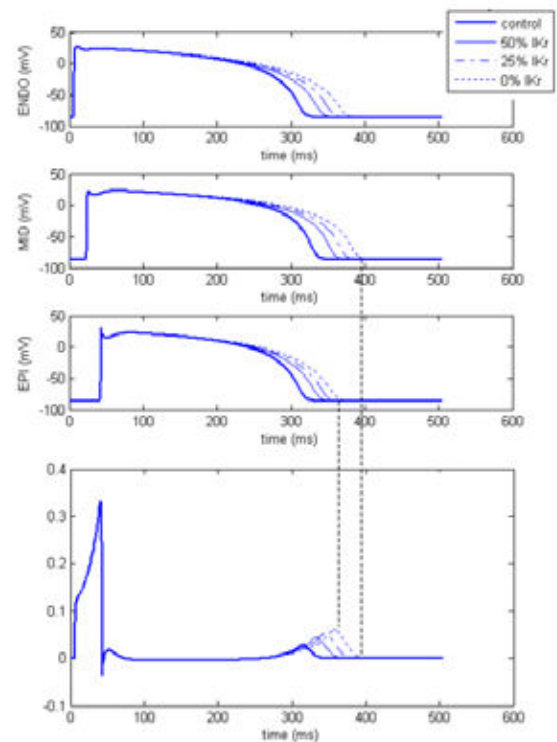


Figure 6. QT intervals of LQT2 are lengthened (control = 335 ms, $50\%I_{Kr}$ = 358 ms, $25\%I_{Kr}$ = 372 ms and $0\%I_{Kr}$ = 388 ms). The T-wave is widened (the peak-end duration of the T-wave is 24 ms for control, 29 ms for $50\%I_{Kr}$, 31 ms for $25\%I_{Kr}$, and 34 ms for $0\%I_{Kr}$) and increased in the amplitude.

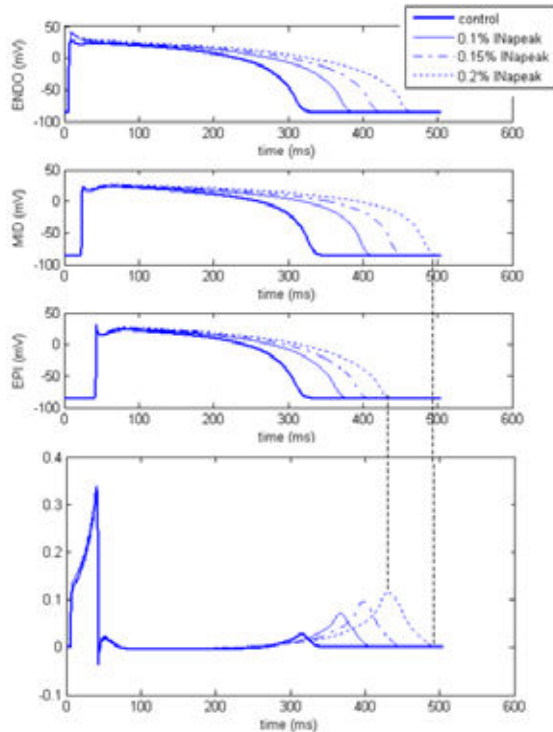


Figure 7. QT intervals of LQT3 are lengthened (control = 335 ms, $0.1\%I_{Napeak}$ = 400 ms, $0.15\%I_{Napeak}$ = 439 ms and $0.2\%I_{Napeak}$ = 483 ms). The T-wave is widened (the peak-end duration of the T-wave is 24 ms for control, 37 ms for $0.1\%I_{Napeaks}$, 45 ms for $0.15\%I_{Napeaks}$, and 56 ms for $0.2\%I_{Napeak}$) and increased in the amplitude.

4. Conclusions

In this paper, we used both the LRd and the TNNP models to simulate APs and QT-intervals of ECG. The QT-interval computed from the TNNP model is closer to the clinical data of normal human hearts under control conditions. The model simulated changes in the QT intervals and changes in the profiles of the T-waves are all fitting well with clinical observations. These simulations establish a causative link between changes in ECG features and gene mutations. The developed models can serve as assistant patterns to study the underlying relationship between morphology of ECG and pathologic and pharmacological changes of APs. In future, we plan to extend the TNNP model into a 2D tissue or a 3D anatomical model of human ventricle to simulate effects of LQT on reentry and drug actions on LQT syndrome.

Acknowledgements

This work was supported by the National Nature Science Foundation of China (NSFC) under grant No. 60571025.

References

- [1] Kazutaka Gima, Yoram Rudy. Ionic Current Basis of Electrocardiographic Waveforms: A Model Study. *Circulation Research* 2002;90:889-896.
- [2] H.Zhang, J.C.Hancox. In silico study of action potential and QT interval shortening due to loss of inactivation of the cardiac rapid delayed rectifier potassium current. *Biochemical and Biophysical Research Communication* 2004;322:693-699.
- [3] G Seemann, DL Weiß, FB Sachse, O Dössel. Simulation of the Long-QT Syndrome in a Model of Human Myocardium. *Computer in Cardiology* 2003;30:287-290.
- [4] K.H.W.J.ten Tusscher, D.Noble, P.J.Noble, A.V. Panfilov. A model for human ventricular tissue. *AM J Physiol Heart Circ Physiol* 2004;286:1573-1589.
- [5] GR. Li, JL.Feng, LX.Yue, M. Carrier. Transmural Heterogeneity of Action Potentials and Ito in Myocytes Isolated from The Human Right Ventricle. *AM J Physiol Heart Circ Physiol* 1998;275:369-377.
- [6] C.E.Chiang, D.M.Roden. The Long QT Syndrome: Genetic Basis and Clinical Implications. *J AM Coll Cardiol* 2000;36:1-12.
- [7] Li Zhang et.al. Spectrum of ST-T-Wave Patterns and Repolarization Parameters in Congenital Long-QT Syndrome. *Circulation* 2000;102:2849-2855.

Address for correspondence

Kuanquan Wang
 Bio-computing Research Centre
 School of Computer Science and Technology
 Harbin Institute of Technology
 No.92 West Dazhi Street, Nangang District, Harbin City,
 150001, Heilongjiang Province, China
 E-mail : wangkq@hit.edu.cn